

Perturbation Theoretical Approach to the Generalized Kubelka-Munk Problem in Nonhomogeneous Optical Media

ANDREAS MANDELIS* and J. P. GROSSMAN

Photothermal and Optoelectronic Diagnostics Laboratory, Department of Mechanical Engineering, University of Toronto, Toronto M5S 1A4, Canada

The generalized Kubelka-Munk problem is considered in nonhomogeneous optical media with arbitrary depth-dependent absorption and scattering coefficients. Regular perturbation theory is applied to the resulting Riccati equation, and explicit expressions are derived for the diffuse reflectance and transmittance of a finite thickness layer. The first-order perturbation solution to the problem with exponentially distributed absorption and scattering coefficients is presented, and the implications for the quantitative study of nonhomogeneous optical media, such as powdered layers, are discussed.

Index Headings: Reflectance spectroscopy; Transmittance spectroscopy; Analytical methods; Optics; Spectroscopic techniques.

INTRODUCTION

The Kubelka-Munk (KM) theory¹ has found wide acceptance and applicability in applied spectroscopy due to its ability to relate the diffuse reflectance and transmittance signals to the absorption and scattering coefficients of a light-diffusing material. The most successful use of the KM theory is through the "Kubelka-Munk function":

$$F(R_\infty) \equiv \frac{(1 - R_\infty)^2}{2R_\infty} = \frac{k}{s} \quad (1)$$

where R_∞ is the diffuse reflectance of an infinitely thick sample, $k(\lambda)$ is its absorption coefficient, and $s(\lambda)$ is its scattering coefficient, both functions of the wavelength of the incident radiation and both assumed to be independent of depth in the material.² The simple KM theory is further readily extendable to the case where both $k = k(x)$ and $s = s(x)$ are functions of depth with the same functional dependence:

$$k(x) = k_0 f(x) \quad (2)$$

and

$$s(x) = s_0 f(x). \quad (3)$$

This special case can be encountered with a powdered sample, when the packing density varies with depth. Then both s and k may be proportional to the density ρ

$$f(x) = \rho(x) \quad (4)$$

so that the ratio k/s will be constant and independent of x . Recent experimental results with two types of silica powders (Cab-O-Sil and Li Chrosorb)³ have shown concrete evidence that variations in packing density of the powder may lead to $k(x)$ and $s(x)$ depth profiles which are quite different from each other, and for which no simple relation, such as Eqs. 2 and 3, may be found. For example, the diffuse reflectance infrared Fourier transform (DRIFT) spectra of Cab-O-Sil powders of thickness d at $\bar{\nu} = 2247 \text{ cm}^{-1}$, a characteristic absorption peak due to the chromophore-CN, following treatment with the aminosilane DMP-CN, was found to give the best fit to a heuristic numerical KM model with $K(x) = 2k(x)$ and $S(x) = 2s(x)$, where

$$K(x) = C + B \exp[-A(1 - x/d)] \quad (5a)$$

and

$$S(x) = C' + B' \exp[-A'(1 - x/d)]. \quad (5b)$$

The assumption of exponential depth profiles of K and S can be justified, somewhat tenuously, if one assumes that the powder density gradient is proportional to the density itself at a given depth x and that the powder size increases with depth (i.e., the density decreases)—a typical situation arising after ultrasonic (mechanical) agitation of the powdered system.³

For the dependences of Eqs. 5a and 5b, there can be no analytical solution to the KM problem. This is also true for all functional forms of K and S , such that

$$S(x) \neq \text{const.} \times K(x). \quad (6)$$

The reason why this statement is true is that the two coupled KM equations for the light flux in the forward direction, $I(x)$, and in the back-scattered direction, $J(x)$ (see Fig. 1), can be shown to be equivalent to the general Riccati equation, which has no known general closed-form solution under the condition of Eq. 6. If it did, that solution would be equivalent to a quadrature solution for all linear second-order equations, which has never been discovered.⁴

Lin and Kan⁵ considered the KM problem with an exponential $k(x)$ dependence of the type described in

Received 6 December 1991.

* Author to whom correspondence should be sent.

Eq. 5a, while the scattering coefficient s was assumed to be depth independent, without further justification. Under these conditions, those authors were able to find an analytical solution in terms of Kummer's confluent hypergeometric equation. The solution given in terms of Kummer's serial function must, however, lie within a specified radius of convergence, a typical property of series solutions to ordinary differential equations. In that particular case the solution was convergent for all values of the depth parameter x , with slowest convergence for values of x near the sample surface.

An empirical approach to the fully generalized KM problem was adopted by Moser-Boroumand.³ The powdered sample was theoretically divided into thin layers, and the values of K_j and S_j were assumed to be constant within the j th layer. In each layer the corresponding value $K_j = K(x_j)$, $S_j = S(x_j)$ was determined from Eqs. 5, so that the contributions to the diffuse reflectance, R , and transmittance, T , from the local values R_j and T_j , were

$$R_j = \frac{\sinh(b_j S_j d_j)}{a_j \sinh(b_j S_j d_j) + b_j \cosh(b_j S_j d_j)} \quad (7a)$$

and

$$T_j = \frac{b_j}{a_j \sinh(b_j S_j d_j) + b_j \cosh(b_j S_j d_j)} \quad (7b)$$

for all layers but the deepest one ($j = n$). For that layer, the diffuse reflectance was written as

$$R_n = \frac{1 - R_g [a_n - b_n \coth(b_n S_n d_n)]}{a_n + b_n \coth(b_n S_n d_n) - R_g}. \quad (8)$$

In Eqs. 7 and 8, d_j is the thickness of the j th layer; $a_j \equiv 1 + K_j/S_j$; $b_j = (a_j^2 - 1)^{1/2}$; and R_g is the reflectance of the sample backing material (substrate or container). The values of A , A' , and B' in Eqs. 5a and 5b were adjusted through the best fit of the properly summed up total theoretical reflectance R to the DRIFT data as a function of the average absorption coefficient $\langle k \rangle$ for the Cab-O-Sil system. The values of C and C' were set equal to zero, and B was renormalized to unity.

The above empirical approach, albeit practically quite satisfactory, tacitly assumes via Eqs. 7 and 8 that each layer is decoupled from those above it and below it through a zero boundary reflectance condition, except for the n th layer. That this is only a rather crude approximation to the generalized KM problem is borne out by the fact that the original differential equation was replaced by the sum of the equations for each strip (j), each with a different set of constants (a_j , b_j). This operation based on the linearity property is, generally, not allowed with nonlinear equations, such as the generalized KM (Riccati) equation.

For these reasons we present the first mathematically rigorous formulation and solution of the generalized KM problem in terms of Regular Perturbation Theory, in which the zeroth-order solution is obtainable in terms of the well-known conventional KM solution. Analytical expressions for general $K(x)$ and $S(x)$ profiles may be obtained, while the perturbation formalism can be shown⁴ to be convergent for all values of x , not limited by local

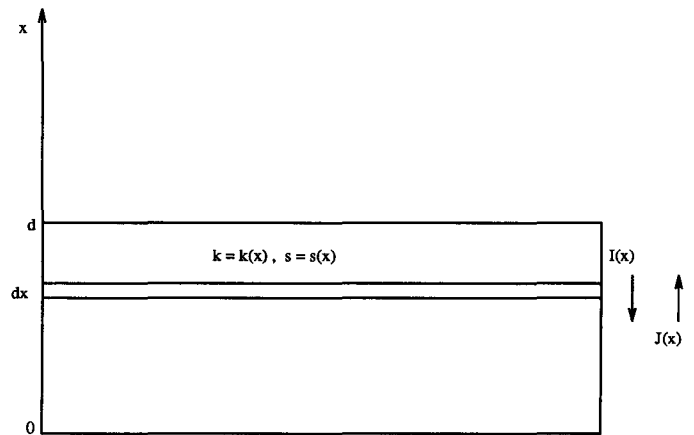


FIG. 1. One-dimensional geometry for the generalized KM problem.

considerations of a radius of convergence—a severe constraint of series solutions for many functional forms.

THE GENERALIZED KM EQUATION

Considering a strip dx in Fig. 1, the optical energy flux balance equations in the forward ($d \rightarrow 0$) and the reverse (back-scattered, $0 \rightarrow d$) directions can be expressed in terms of $K(x) = 2k(x)$

$$-\frac{d}{dx}I(x) = -[K(x) + S(x)]I(x) + S(x)J(x) \quad (9)$$

$$\frac{d}{dx}J(x) = -[K(x) + S(x)]J(x) + S(x)I(x). \quad (10)$$

The wavelength dependences of $K(x)$ and $S(x)$ have been suppressed, since they can be carried along without altering the depth dependences. Upon definition of the parameters:

$$a(x) \equiv 1 + \frac{K(x)}{S(x)} \quad (11)$$

and

$$r(x) \equiv \frac{J(x)}{I(x)}, \quad (12)$$

addition and rearrangement of Eqs. 9 and 10 yields

$$\frac{d}{dx}r(x) = S(x)[r^2(x) - 2a(x)r(x) + 1] \quad (13)$$

with the boundary conditions:

$$r(d) = R, \quad r(0) = R_g (= 0 \text{ for simplicity}). \quad (14)$$

Equation 13 is the generalized Riccati equation. The substitution

$$r(x) = -\frac{dw(x)/dx}{S(x)w(x)} \quad (15)$$

gives the linear second-order equation:

$$\frac{d^2}{dx^2}w(x) + p_1(x)\frac{d}{dx}w(x) + p_0(x)w(x) = 0 \quad (16)$$

where

$$p_1(x) \equiv 2a(x)S(x) - \frac{d}{dx} \ln S(x) \quad (17a)$$

and

$$p_0(x) \equiv S^2(x). \quad (17b)$$

A further change in variable according to:

$$w(x) = v(x) \exp \left[-\frac{1}{2} \int^x p_1(y) dy \right] \quad (18)$$

transforms the generalized Riccati equation into

$$\frac{d^2}{dx^2} v(x) + \left[p_0(x) - \frac{1}{2} \frac{d}{dx} p_1(x) - \frac{1}{4} p_1^2(x) \right] v(x) = 0. \quad (19)$$

At the same time, it is easy to show that the original boundary conditions (Eq. 14) must be replaced by

$$v'(0) = \frac{1}{2} v(0) p_1(0) \quad (20a)$$

and

$$\frac{v'(d)}{v(d)} = \frac{1}{2} p_1(d) - RS(d). \quad (20b)$$

It is, therefore, apparent that the expression for the total diffuse reflectance R can be obtained via the second boundary condition, provided that Eq. 19 can be explicitly solved. Equations 19 and 20 comprise the generalized Kubelka-Munk problem.

In the limit of constant $a(x)$ (i.e., if S and K are both constant, or they have the same functional dependence), $r(x)$ is well known²

$$r(x) = \frac{\sinh[b_0 Q(x)]}{a_0 \sinh[b_0 Q(x)] + b_0 \cosh[b_0 Q(x)]} \quad (21)$$

where

$$a_0 = 1 + \frac{K_0 f(x)}{S_0 f(x)} = 1 + \frac{K_0}{S_0} \quad (22a)$$

$$b_0 = (a_0^2 - 1)^{1/2} \quad (22b)$$

and

$$Q(x) \equiv \int_0^x S(y) dy. \quad (23)$$

Now, Eq. 15 yields

$$w(x) = \exp \left[- \int_0^x S(y) r(y) dy \right] \\ = \frac{1}{2} [(a_0 + b_0) e^{b_0 Q(x)} - (a_0 - b_0) e^{-b_0 Q(x)}] e^{-a_0 Q(x)}. \quad (24)$$

Finally, Eq. 18 gives the solution to the generalized KM problem when $a(x) = a_0$:

$$v_0(x) = \frac{1}{2b_0 S^{1/2}(x)} [(a_0 + b_0) e^{b_0 Q(x)} - (a_0 - b_0) e^{-b_0 Q(x)}]. \quad (25)$$

In a tedious but straightforward manner, Eq. 20b becomes:

$$R = \frac{p_1(d)}{2S(d)} - \frac{v'_0(d)}{S(d)v_0(d)} \\ = \frac{\sinh[b_0 Q(d)]}{a_0 \sinh[b_0 Q(d)] + b_0 \cosh[b_0 Q(d)]} \quad (26)$$

as expected from the hyperbolic solutions to the conventional KM problem.

REGULAR PERTURBATION THEORY OF THE GENERALIZED KM PROBLEM

The derived Eq. 25 represents the exact solution to what will be now considered the zeroth-order (leading term) in a perturbation expansion of the fully generalized KM problem, Eqs. 19 and 20. The pertinent small parameter ϵ can be defined in terms of the particular functional dependences adopted for $K(x)$ and $S(x)$. In general, and in agreement with the requirement that the solution to Eq. 19 should obey

$$\lim_{a(x) \rightarrow a_0} v(x) = \lim_{\epsilon \rightarrow 0} v(x; \epsilon) = v_0(x), \quad (27)$$

one may write:

$$a(x) = a_0 + \epsilon V(x). \quad (28)$$

Equation 17a now becomes

$$p_1(x) = p_1^{(0)}(x) + \epsilon p_1^{(1)}(x) \quad (29a)$$

where

$$p_1^{(0)}(x) = 2a_0 S(x) - \frac{d}{dx} \ln S(x) \quad (29b)$$

$$p_1^{(1)}(x) = 2S(x)V(x). \quad (29c)$$

Equation 19 is replaced by

$$v''(x) + [G^{(0)}(x) - \epsilon Y(x) - \epsilon^2 X(x)]v(x) = 0 \quad (30)$$

with the following definitions:

$$G^{(0)}(x) \equiv p_0(x) - \frac{1}{2} [p_1^{(0)}(x)]' - \frac{1}{4} [p_1^{(0)}(x)]^2 \quad (31)$$

$$Y(x) \equiv \frac{1}{2} \{ [p_1^{(1)}(x)]' + p_1^{(0)}(x)p_1^{(1)}(x) \} \\ = S(x)[a_0 p_1^{(1)}(x) + dV(x)/dx] \quad (32)$$

and

$$X(x) \equiv S^2(x)V^2(x). \quad (33)$$

Now we assume a perturbation expansion of the form

$$v(x) = \sum_{m=0}^{\infty} \epsilon^m \Psi_m(x). \quad (34)$$

Substitution of Eq. 34 in 30 and separation of the various orders results in the following iterative system of equations for calculating the successive terms of the expansion:

$$\Psi''_0(x) + G^{(0)}(x)\Psi_0(x) = 0; \quad O(1) \quad (35a)$$

$$\Psi''_1(x) + G^{(0)}(x)\Psi_1(x) = Y(x)\Psi_0(x); \quad O(\epsilon) \quad (35b)$$

$$\begin{aligned} & \vdots \\ \Psi''_n(x) + G^{(0)}(x)\Psi_n(x) &= Y(x)\Psi_{n-1}(x) + X(x)\Psi_{n-2}(x); \\ & O(\epsilon^n), n \geq 2. \end{aligned} \quad (35c)$$

The boundary conditions (Eq. 20) may be recast in the perturbational formalism upon setting

$$R = \sum_{m=0}^{\infty} \epsilon^m R_m. \quad (36)$$

Equations 20 and 36 give for the various orders:

$$\left. \begin{aligned} \Psi'_0(0) &= \frac{1}{2} p_1^{(0)}(0) \Psi_0(0) \\ \Psi'_0(d) &= \left[\frac{1}{2} p_1^{(0)}(d) - S(d) R_0 \right] \Psi_0(d) \end{aligned} \right\}; O(1) \quad (37a)$$

$$\left. \begin{aligned} \Psi'_1(0) &= \frac{1}{2} [p_1^{(0)}(0) \Psi_1(0) + p_1^{(1)}(0) \Psi_0(0)] \\ \Psi'_1(d) &= \left[\frac{1}{2} p_1^{(0)}(d) - S(d) R_0 \right] \Psi_1(d) \\ &+ \left[\frac{1}{2} p_1^{(1)}(d) - S(d) R_1 \right] \Psi_0(d) \end{aligned} \right\}; O(\epsilon) \quad (37b)$$

$$\left. \begin{aligned} & \vdots \\ \Psi'_n(0) &= \frac{1}{2} [p_1^{(0)} \Psi_n(0) + p_1^{(1)}(0) \Psi_{n-1}(0)] \\ \Psi'_n(d) &= \left[\frac{1}{2} p_1^{(0)}(d) - S(d) R_0 \right] \Psi_n(d) \\ &+ \left[\frac{1}{2} p_1^{(1)}(d) - S(d) R_1 \right] \Psi_{n-1}(d) \\ &- S(d) [R_2 \Psi_{n-2}(d) \\ &+ R_3 \Psi_{n-3}(d) + \dots \\ &+ R_n \Psi_0(d)]; n \geq 2 \end{aligned} \right\}; O(\epsilon^n). \quad (37c)$$

It should be noticed that the zeroth-order Eq. 35a, subject to the boundary conditions (Eq. 37a), is identical to the conventional KM problem with constant $a(x) = a_0$, the solution of which is given by Eq. 25:

$$\Psi_0(x) = v_0(x) \quad (38)$$

and $R_0 = R$ in Eq. 26. Now the first-order perturbational function $\Psi_1(x)$ can be determined from Eqs. 35b and 37b with the use of the technique of variation of parameters and the definitions:

$$F_{\pm}(x) \equiv \frac{e^{\pm b_0 Q(x)}}{S^{1/2}(x)}. \quad (39)$$

The solution (complementary and inhomogeneous) of Eq. 35b is

$$\begin{aligned} \Psi_1(x) &= A_1 F_+(x) + A_2 F_-(x) \\ &+ \frac{1}{2b_0} [F_+(x) H_-(x) - F_-(x) H_+(x)] \end{aligned} \quad (40)$$

where A_1 and A_2 are integration constants to be determined from the boundary conditions, Eqs. 37b, and

$$H_{\pm}(x) \equiv \int^x Y(y) \Psi_0(y) F_{\pm}(y) dy. \quad (41)$$

Following some tedious algebraic manipulations, one obtains for the first-order perturbational KM function:

$$\begin{aligned} \Psi_1(x) &= \frac{1}{2b_0 S^{1/2}(x)} \\ &\times \{ a_0 \sinh[b_0 Q(x)] + b_0 \cosh[b_0 Q(x)] \\ &+ (a_0 - b_0) [a_0 M_-(x) + b_0 M_+(x) - b_0 e^{-b_0 Q(x)} V(0)] \\ &- e^{-b_0 Q(x)} [H_+(x) - H_+(0)] \} \end{aligned} \quad (42)$$

where

$$M_{\pm}(x) \equiv e^{b_0 Q(x)} H_-(x) \pm e^{-b_0 Q(x)} H_-(0). \quad (43)$$

Although higher orders are, in principle, straightforward, in practice they result in very complicated algebraic expressions. Extensive numerical modeling of the present formalism with specific $V(x)$ dependences, including $O(\epsilon^2)$, has shown that for wide ranges of $\epsilon \leq 1$ the ϵ^2 terms incur a correction of less than 3% to the $O(\epsilon)$ contribution [$0.001 \leq \epsilon \leq 1$]. Therefore, we decided not to extend the perturbation expansion beyond $O(\epsilon)$, having numerically proven that the correction effected by higher orders is well within experimental uncertainty in many applications to applied spectroscopy.

DIFFUSE REFLECTANCE AND TRANSMITTANCE FUNCTIONS

Once the perturbation functions $\Psi_j(x)$ are determined, Eq. 20b may be used to express the total diffuse reflectance from an inhomogeneous sample of thickness d :

$$R = a_0 + \epsilon V(d) - \frac{1}{S(d)} \left\{ \frac{1}{2} \frac{S'(d)}{S(d)} + \frac{\sum_{m=0}^{\infty} \epsilon^m \Psi'_m(d)}{\sum_{m=0}^{\infty} \epsilon^m \Psi_m(d)} \right\}. \quad (44)$$

For finite-thickness layers, the diffuse transmittance can also be calculated from Eqs. 9, 15, and 18 as follows:

From Eqs. 15 and 18

$$r(x) S(x) = \frac{1}{2} p_1(x) - \frac{1}{v(x)} \frac{dv(x)}{dx}. \quad (45)$$

Now Eq. 9 becomes

$$\begin{aligned} \frac{dI(x)}{I(x)} &= \left[a(x) S(x) - \frac{1}{2} p_1(x) \right] dx + \frac{dv(x)}{v(x)} \\ &= \left\{ a_0 S(x) - \frac{1}{2} p_1^{(0)}(x) \right. \\ &+ \left. \epsilon \left[V(x) S(x) - \frac{1}{2} p_1^{(1)}(x) \right] \right\} dx + \frac{dv(x)}{v(x)}. \end{aligned} \quad (46)$$

Equation 46 is easily simplified:

$$\frac{dI(x)}{I(x)} = \left[\frac{S'(x)}{2S(x)} \right] dx + \frac{dv(x)}{v(x)}$$

or, upon integration between $x = d$ (surface) and $x = 0$ (sample/substrate interface):

$$\frac{I(0)}{I(d)} \equiv T = \left[\frac{S(0)}{S(d)} \right]^{1/2} \left[\frac{v(0)}{v(d)} \right]. \quad (47)$$

Finally, this expression can be written in terms of the perturbation expansion, Eq. 34:

$$T = \left[\frac{S(0)}{S(d)} \right]^{1/2} \frac{\sum_{m=0}^{\infty} e^m \Psi_m(0)}{\sum_{m=0}^{\infty} e^m \Psi_m(d)}. \quad (48)$$

Setting $V(x) = 0$ in Eqs. 44 and 48, along with Eq. 38, results in the conventional KM expressions (Eqs. 7a and 7b), as expected.

A SPECIAL $K(x)$, $S(x)$ CASE

In this section we will show the application of the perturbational KM solution developed in this work to a particularly useful functional dependence of the coefficients $K(x) = 2k(x)$ and $S(x) = 2s(x)$ —namely, exponential decay profiles. Such depth profiles were considered in earlier studies.^{3,6} If $K(x)$ and $S(x)$ are assumed to have the same functional depth dependence, then $a(x) = a_0$, and this relation implies $V(x) = 0$. It is easy to see that the perturbation expression for R becomes

$$R = a_0 - \frac{1}{S(d)} \left[\frac{1}{2} \frac{S'(d)}{S(d)} + \frac{\Psi'_0(d)}{\Psi_0(d)} \right]. \quad (49)$$

Equation 49 can be easily transformed to the well-known Eq. 26 upon use of Eq. 38. Similarly, Eq. 48 gives

$$T = \left[\frac{S(0)}{S(d)} \right]^{1/2} \frac{\Psi_0(0)}{\Psi_0(d)} = \frac{b_0}{a_0 \sinh[b_0 Q(d)] + b_0 \cosh[b_0 Q(d)]}, \quad (50)$$

as expected.

In the generalized case where $K(x)$ and $S(x)$ have similar (exponential) functional dependences on x , but different depth profiles

$$S(x) = S_0 e^{-B(d-x)} \quad (51a)$$

and

$$K(x) = K_0 e^{-A(d-x)}, \quad (51b)$$

assuming that $K_0 < S_0$, the perturbational representation of $a(x)$, Eq. 28, is written as:

$$\epsilon = K_0/S_0; \quad V(x) = \exp[(B-A)(d-x)] - 1. \quad (52)$$

The rest of the perturbation functions are

$$Y(x) = S_0 [2a_0 S_0 (e^{-A(d-x)} - e^{-B(d-x)}) - (B-A)e^{(B-A)(d-x)}] e^{-B(d-x)}, \quad (53)$$

$$X(x) = S_0^2 [e^{-A(d-x)} - e^{-B(d-x)}]^2, \quad (54)$$

and

$$Q(d) = \frac{S_0}{B} (1 - e^{-Bd}). \quad (55)$$

Now we are left with the evaluation of the first-order perturbation integrals $H_{\pm}(x)$ and $M_{\pm}(x)$ (see Eq. 42). After considerable algebra we obtain:

$$H_-(x) = \frac{1}{4b_0} \left\{ (a_0 + b_0) e^{-b_0 q} \times [2a_0 S_0 (A^{-1} e^{-A(d-x)} - B^{-1} e^{-B(d-x)}) + e^{(B-A)(d-x)}] - (a_0 - b_0) e^{b_0 q} \times \left(\frac{2(a_0 + b_0) S_0 J_1 [2b_0 (S_0/B) e^{-B(d-x)}]}{B [2b_0 (S_0/B)]^{A/B}} + \{(a_0/b_0) + e^{(B-A)(d-x)}\} \times \exp[-2b_0 (S_0/B) e^{-B(d-x)}] \right) \right\} \quad (56)$$

where

$$q = \left(\frac{S_0}{B} \right) e^{-Bd} \quad (57a)$$

and

$$J_1(z) = \begin{cases} z^{A/B} \sum_{m=0}^{\infty} \frac{(-1)^m}{m!} \left[\frac{z^m}{(A/B) + m} \right]; & (\text{Taylor}; z < 1) \\ (B/A) z^{A/B} e^{-z} \times \left(1 + \sum_{m=1}^{\infty} \frac{z^m}{[(A/B) - 1][(A/B) - 2] \cdots [(A/B) - m]} \right); & (\text{Asymptotic}; z \gg 1). \end{cases} \quad (57b)$$

Similarly:

$$H_+(x) = \frac{1}{4b_0} \left\{ (a_0 + b_0) e^{-b_0 q} \times \left(\frac{2(a_0 - b_0) S_0 J_2 [2b_0 (S_0/B) e^{-B(d-x)}]}{B [2b_0 (S_0/B)]^{A/B}} - \{(a_0/b_0) - e^{(B-A)(d-x)}\} \times \exp[2b_0 (S_0/B) e^{-B(d-x)}] \right) - (a_0 - b_0) e^{b_0 q} \times [2a_0 S_0 (A^{-1} e^{-A(d-x)} - B^{-1} e^{-B(d-x)}) + e^{(B-A)(d-x)}] \right\} \quad (58)$$

where

$$\begin{aligned}
& J_2(z) \\
& = \begin{cases} z^{A/B} \sum_{m=0}^{\infty} \frac{1}{m!} \left[\frac{z^m}{(A/B) + m} \right]; & \text{(Taylor; } z < 1) \\ (B/A)z^{A/B} e^z \left(1 + \sum_{m=1}^{\infty} (-1)^m \right. \\ \quad \left. \times \frac{z^m}{[(A/B) - 1][(A/B) - 2] \cdots [(A/B) - m]} \right); & \text{(Asymptotic; } z \gg 1). \end{cases} \quad (59)
\end{aligned}$$

Once the two fundamental functions $H_+(x)$ and $H_-(x)$ are defined and calculated for this special depth profiling case, Eq. 43 may be used to calculate $M_{\pm}(x)$. Then R and T can be calculated up to $O(\epsilon)$ from Eqs. 44 and 48, noting that $V(d) = 0$ for the particular choice of Eq. 52 for $V(x)$. These results were examined via computer simulations for several ranges of the parameters. Under the above conditions, the perturbation expressions for the diffuse reflectance and transmittance up to first-order for the profiles of Eqs. 51a and 51b are:

$$R = a_0 - \frac{1}{S_0} \left[\frac{(1 + \epsilon)D'(d) + \epsilon E'(d)}{(1 + \epsilon)D(d) + \epsilon E(d)} \right] \quad (60)$$

and

$$T = \frac{(1 + \epsilon)D(0) + \epsilon E(0)}{(1 + \epsilon)D(d) + \epsilon E(d)} \quad (61)$$

where

$$D(x) \equiv \frac{1}{2b_0} (a_0 \sinh[b_0 Q(x)] + b_0 \cosh[b_0 Q(x)]) \quad (62)$$

and

$$D'(x) = \frac{1}{2} S(x) (a_0 \cosh[b_0 Q(x)] + b_0 \sinh[b_0 Q(x)]). \quad (63)$$

Also:

$$\begin{aligned}
E(x) \equiv & \frac{1}{2b_0} \{ (a_0 - b_0) e^{b_0 q} \\
& \times [a_0 M_-(x) + b_0 M_+(x) - b_0 e^{-b_0 q} V(0)] \\
& - e^{-b_0 q} [H_+(x) - H_+(0)] \} \quad (64)
\end{aligned}$$

and

$$\begin{aligned}
E'(x) = & \frac{1}{2} S(x) \{ (a_0 - b_0) e^{b_0 q} \\
& \times [a_0 M_+(x) + b_0 M_-(x) + b_0 e^{-b_0 q} V(0)] \\
& + e^{-b_0 q} [H_+(x) - H_+(0)] \}. \quad (65)
\end{aligned}$$

Figure 2 shows reflectance and transmittance curves, Eqs. 60 and 61, for a sample of thickness $d = 3$ mm, in which identical exponential depth profiles $S(x)$ and $K(x)$ exist, with only the pre-exponential factor ratio K_0/S_0 varying.

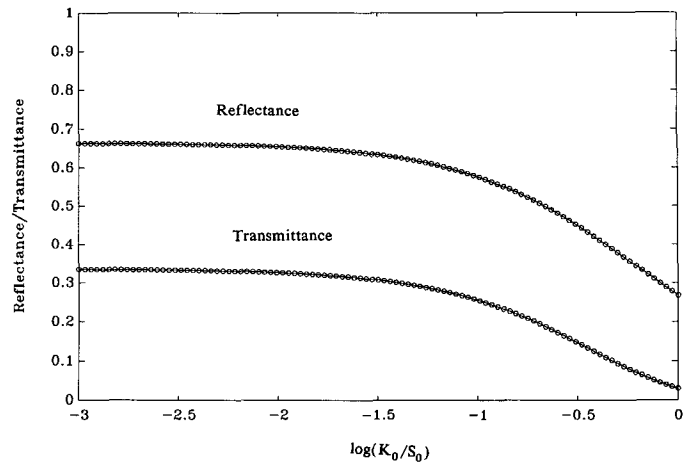


FIG. 2. Conventional (—) and perturbational (—○—) KM behavior of a sample with $d = 0.3$ cm, $A = B = 3$ mm $^{-1}$, and $S_0 = 10$ mm $^{-1}$.

Also plotted are the conventional KM curves for constant absorption and scattering coefficients (Eqs. 7a and 7b) with zero background reflectance condition. It can be seen that the two sets of curves are identical over three orders of magnitude in $\epsilon = K_0/S_0$. The total number of terms used in evaluating the functions $H_{\pm}(x)$ in Eqs. 56–59 were 61. This figure bears out the fact that the original KM functions can adequately describe constant and depth-variable K and S profiles of identical functional dependence.² It is also a proof that the regular perturbational approach used here is well behaved in the limits of both these cases ($\epsilon = 0$ or $A = B$ in Eqs. 51a and 51b).

Figure 3 shows diffuse reflectance and transmittance curves as functions of sample thickness d for several values of ϵ and widely different exponential decay profiles of $K(x)$ and $S(x)$ into the sample. Substantial decreases in the saturation values for R are observed with increasing ϵ (i.e., with increasing K_0) since $S_0 = 10$ cm $^{-1}$ throughout these simulations. This is expected, since less light is available for reflection with increased absorption. Similarly, the transmittance decreases strongly with increasing K_0 . The total number of terms used for the functions $H_{\pm}(x)$ was 61. Although quite adequate for most of the d -range sampled, there are some values of d for which the R and T curves exhibit sharp, localized vertical asymptotes. These divergences recover very quickly: typically two or three such divergences can appear in Fig. 3 with recovery range $\sim d_j \pm 0.1d_j$. They have been traced to the need for many more terms in representing $H_{\pm}(d)$ for certain values of d where the denominators in Eqs. 60 and 61 are such that $D(d)$ and $E(d)$ change signs. In order to avoid long computation times and computer use, we found that it is possible to eliminate these local divergences through direct manipulation of the curves themselves, rather than through inclusion of a much larger number of terms near the neighborhood of the asymptotes. This strategy is very efficient, since (1) there is no *a priori* knowledge of where the local divergences will occur for a given R and T curve, and (2) the majority of the data in each curve exhibit well-behaved, convergent values with fewer than 100 terms in the H_{\pm} series. The method utilized to eliminate the asymptotes and thus produce continuous curves such as those of Fig. 3

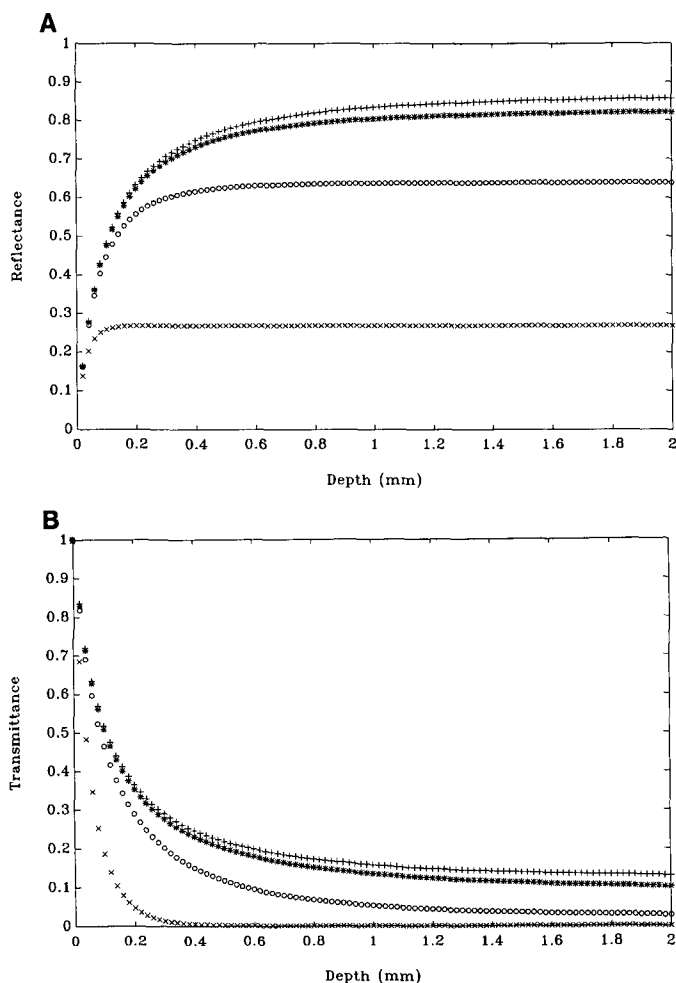


FIG. 3. Diffuse reflectance (A) and transmittance (B) as a function of thickness. Absorption and scattering coefficient depth profiles have parameters $A = 0.1 \text{ mm}^{-1}$, $B = 1.5 \text{ mm}^{-1}$, $S_0 = 10 \text{ mm}^{-1}$. The perturbation parameter $\epsilon = 10^{-3}$ (+ + +); 10^{-2} (* * *); 10^{-1} (O-O-O); and 1 (x-x-x).

was based on modifying each curve $R(d)$ or $T(d)$ to a smooth one representing their envelope. For $R(d)$, for instance, a suitable mapping was generated which maps the curve $y = \frac{1}{d}$ onto $y = R(d)$. The specific mapping used was

$$R(d) \equiv md + b + \frac{k}{d - d_a} \quad (66)$$

for values of d close to the center value d_a at which $R(d)$ exhibited divergence. Using four points p_1, p_2, p_3, p_4 with $p_i \equiv [d_i, R(d_i)]$ and $d_1 < d_2 < d_a < d_3 < d_4$, one obtains four equations in the four variables m, b, k , and d_a . Solving Eq. 66 for these variables, we redefine the smoothed curve as

$$R_s(d) = R(d) - \frac{k}{d - d_a}. \quad (67)$$

This method proved very effective and was incorporated into all further simulations, producing curves of very good continuity. Similar simulations to those of Fig. 3, but with $A = 1.5 \text{ mm}^{-1}$, showed very little change in the obtained profiles of both R and T curves. This effect—

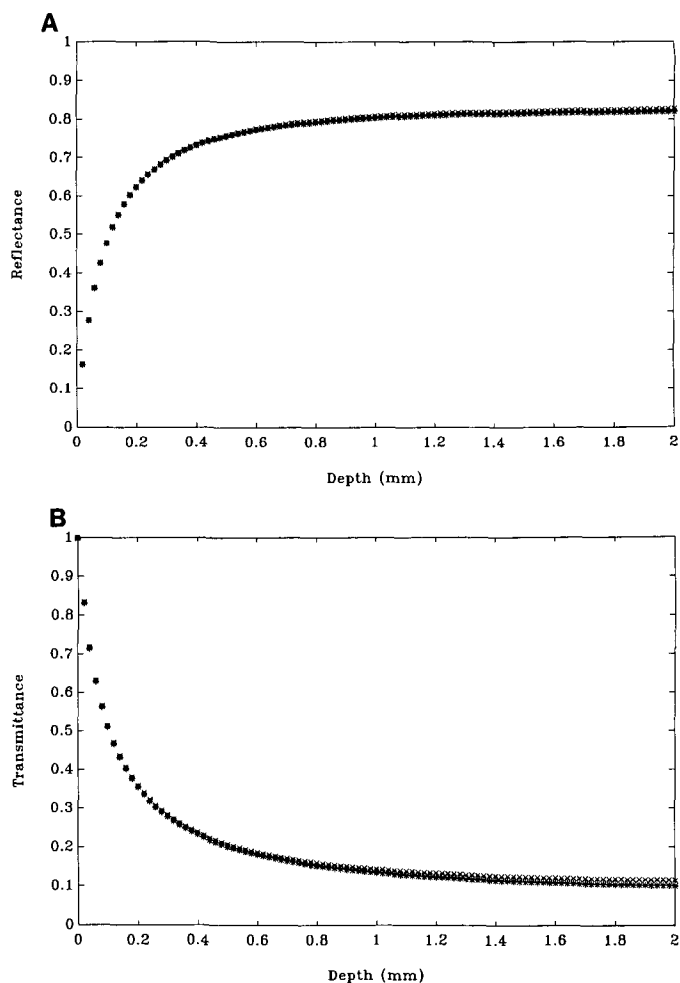


FIG. 4. Diffuse reflectance (A) and transmittance (B) vs. thickness with the absorption profile exponent A as a parameter. $B = 1.5 \text{ mm}^{-1}$, $S_0 = 10 \text{ mm}^{-1}$, $\epsilon = 0.01$. The values for A are: 0.1 (+ + +); 0.5 (* * *); 1.0 (O-O-O); and 1.5 (x-x-x).

namely, the lack of measurable sensitivity of the data to the steepness of the exponential absorption profile—is illustrated in Fig. 4. Marginally higher transmittance is seen for the steepest chosen absorption profile in Fig. 4B. This transmittance enhancement is expected, as the integrated absorbance

$$\langle K \rangle = \frac{1}{d} \int_0^d K(x) dx = \frac{K_0}{Ad} (1 - e^{-Ad}) \quad (68)$$

decreases with $A \gg d^{-1}$. The simulations in Fig. 4 convey the important message that diffuse reflectance profiles are much more strongly dependent on the absolute value of surface and near-surface absorption coefficient, K_0 (see Fig. 3), than on the depth profile of this coefficient. The cause of the apparent insensitivity to the value of A is the fact that $Ad \lesssim 1$ throughout the range of parameters of Fig. 4, so that the sample behaves as optically transparent with $\langle K \rangle \approx K_0$. Figure 5 shows the effect of the variation in A once the $Ad < 1$ condition is relaxed and S_0 and B are fixed. Similar qualitative results were obtained previously by Lin and Kan⁵—namely, enhancement in total diffuse reflectance at a given K_0/S_0 with increased A due to decreased total absorbance, as well as an increase in reflectance and in transmittance with decreased average absorbance $\langle K \rangle d$ (Eq. 68).

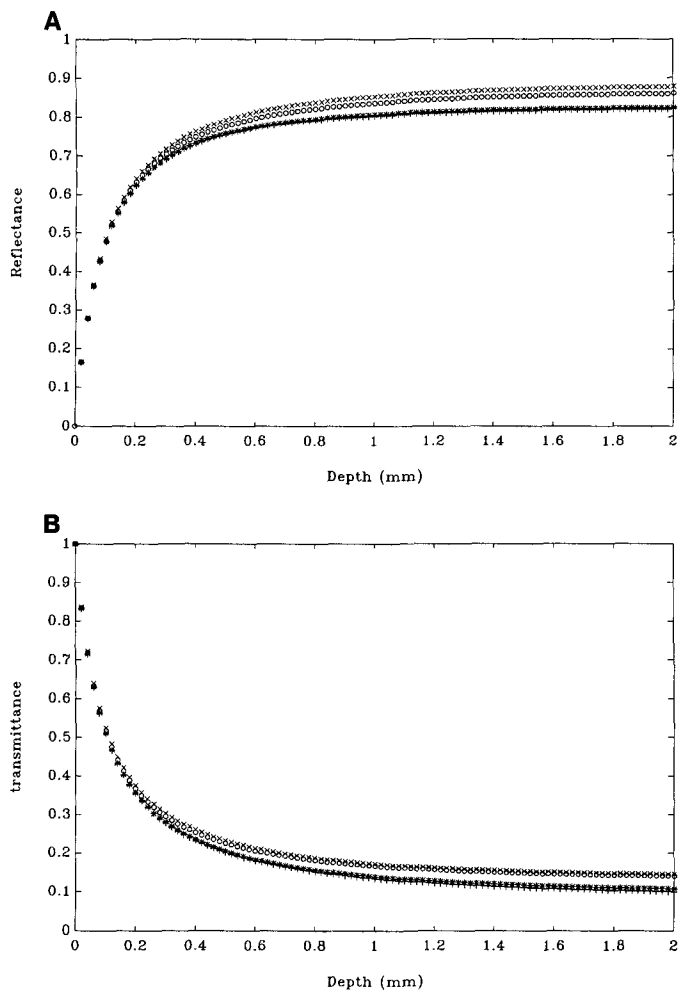


FIG. 5. The effects of the variation in A to the value of diffuse reflectance (A) and transmittance (B) from a sample with $B = 1.5 \text{ mm}^{-1}$, $S_0 = 10 \text{ mm}^{-1}$, and $d = 3 \text{ mm}$. $A = 0.5 \text{ mm}^{-1}$ (++++); 1.0 mm^{-1} (****); 10 mm^{-1} (O-O-O); and 100 mm^{-1} (x-x-x-x).

It is interesting to juxtapose the effect of varying the scattering coefficient profile depth decay rate constant B on the values of R and T as functions of layer thickness (Fig. 6). Low B indicates large scattering throughout the sample thickness, resulting in enhanced R and depressed T . At the other extreme, high B has a dampening effect on scatter and results in the opposite behavior: enhanced diffuse transmittance and decreased reflectance. These trends are consistent with results from a discontinuous approach to the diffuse problem with loosely packed powders, which exhibit a considerable degree of diffuse back-scatter.⁷ It is seen that, even though the range of B values chosen is similar to that of the A values in Fig. 4, the diffuse functions R and T nevertheless exhibit much stronger sensitivity to the scattering coefficient profiles. This result is also due to the well-known fact² that back-scattering affects the reflectance enormously in the $\langle S \rangle d \lesssim 3$ range, as per the conventional KM model. The effect is much less pronounced² with changes in $\langle K \rangle$.

DISCUSSION

Regular perturbation theory has allowed the study of the diffuse function dependence on assumed depth pro-

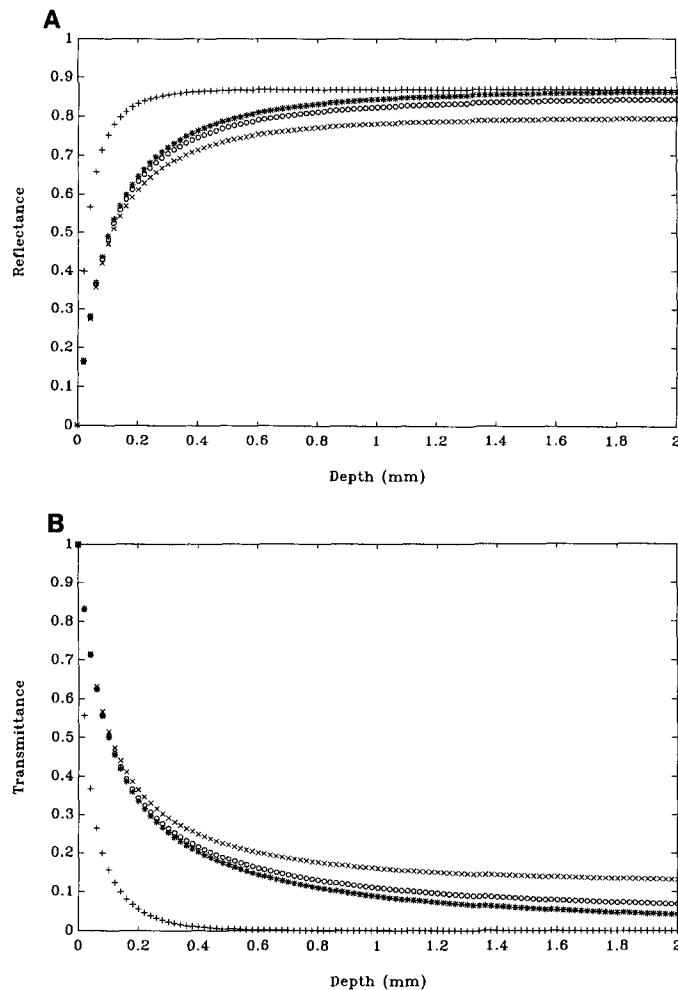


FIG. 6. Diffuse reflectance (A) and transmittance (B) dependence on sample thickness d with B as a parameter. $A = 0.5 \text{ mm}^{-1}$, $\epsilon = 0.01$ and $S_0 = 10 \text{ mm}^{-1}$. The values of B are: 0.1 mm^{-1} (++++); 0.5 mm^{-1} (****); 1.0 mm^{-1} (O-O-O); and 2.0 mm^{-1} (x-x-x-x).

files of the absorption and scattering coefficients. The usefulness of such a treatment becomes apparent in the fitting of experimental data of normalized diffuse reflectance and transmittance signals as functions of the averaged absorptance³ $\langle K \rangle d$. The present theoretical considerations are expected to resolve the inability of the conventional KM theory to fit such data plots³ by providing adjustable parameters A and B , under the (not rigorously justified) assumption of exponential $k(x)$ and $s(x)$ depth profiles. Other types of profiles can be easily handled within the present theoretical framework by accordingly redefining the function $V(x)$ and the parameter ϵ . It is important to emphasize that the perturbational formulation of the KM problem is mathematically rigorous, aimed at providing a justifiable alternative to the empirical numerical approach by Moser-Boroumand.³ At present, it appears that the use of particular depth profiles of $k(x)$ and $s(x)$ is, at best, of little relevance to the actual profiles which may be possibly encountered in nonhomogeneous solid media, such as powders. The exponential profiles and the concomitant mathematical expressions (Eqs. 60-65) could be employed for a specimen to adjust the best fit to the spectroscopic data (R_j and T_j) at each wavelength around an absorption peak, so as

to obtain the local $\bar{\nu}$ values for K_0 , S_0 , A_j , and B_j . A portion of the true experimental depth profile of $k(x)$ and $s(x)$ may thus be reconstructed from the set of all such local values between k_{\max} and k_{\min} , observing that only a region close to the sample surface is probed near a strong absorption peak (i.e., high absorption coefficient, small absorption depth). As k decreases, deeper layers of the sample can be probed, corresponding to a different set of (A_j, B_j) values, while keeping k_0 and s_0 constant (surface values evaluated at k_{\max}). Finally, plotting $k_j(x)$ and $S_j(x)$ vs. depth $x_j = k_j^{-1}(x)$, where x_j corresponds to a pair (A_j, B_j) , will yield reconstructed profiles for the actual $k_j(x)$ and $s_j(x)$, each differential sub-layer represented by local exponential scattering and absorption profiles $S_0 e^{-B_j(d-x_j)}$ and $K_0 e^{-A_j(d-x_j)}$, respectively. Experimental implementation of these ideas will be reported in a future publication.

CONCLUSIONS

A perturbational theoretical treatment of the KM problem has been presented up to first order in the perturbation parameter. The general formalism is shown to be mathematically rigorous and has been applied to the special case of exponential depth profiles for the material absorption and scattering coefficients, and the resulting

diffuse reflectance and transmittance have been studied. Potential applications towards the spectroscopic reconstruction of the absorption and scattering coefficient depth profiles in nonhomogeneous media have been discussed.

ACKNOWLEDGMENTS

The assistance of F. Moser-Boroumand with the original numerical profiles of the perturbation problem and her discovery of the local divergences were decisive in our further optimization of this problem. Her contributions are, therefore, gratefully acknowledged. We wish to thank the Natural Sciences and Engineering Research Council of Canada for partial support of this work.

1. P. Kubelka and F. Munk, *Z. Tech. Physik* **12**, 593 (1931).
2. G. Kortum, *Reflectance Spectroscopy* (Springer-Verlag, Berlin, 1969), Chap. IV.
3. F. Moser-Boroumand, Ph.D. Thesis, Ecole Polytechnique Federale de Lausanne, Switzerland (Dept. of Chemistry, Thesis No. 926, 1991).
4. C. M. Bender and S. A. Orszag, *Advanced Mathematical Methods for Scientists and Engineers* (McGraw-Hill, New York, 1978), Sect. 1.6.
5. T.-P. Lin and H. K. A. Kan, *J. Opt. Soc. Am.* **60**, 1252 (1970).
6. R. W. Kessler, G. Krabicher, S. Uhl, D. Oelkrug, W. P. Hagan, J. Hyslop, and F. Wilkinson, *Opt. Acta* **30**, 1099 (1983).
7. A. Mandelis, F. Boroumand, and H. van den Bergh, *Spectrochim. Acta* **47A**, 943 (1991).